

## Evidence for a 27-My cycle in ocean hypoxia over the last 260 Ma

**Tracking no:** G46735

**Authors:**

Ken Caldeira

**Abstract:**

We find that spectral analyses of the ages of the ten recorded major ocean anoxic events of the past 260 Ma reveal a strong spectral peak at 26.9 My significant at the ~95% confidence level. This cycle matches the periodicities of ~26 to 36 My detected in fluctuations in tectonics, sea levels and climate, in flood-basalt eruptions, and in biotic extinctions. The ages of eight of these anoxic events are correlated with concurrent episodes of extinctions of marine organisms. All ten anoxic intervals are closely associated with the ages of flood-basalt eruptions, suggesting causal connections through volcanic release of greenhouse gases resulting in severe hyperthermal intervals and hypoxia in the oceans.

# Evidence for a 27-Ma cycle in ocean hypoxia over the last 260 Ma

Michael R. Rampino<sup>1,2\*</sup> and Ken Caldeira<sup>3</sup>

<sup>1</sup>*Departments of Biology and Environmental Studies, New York University,  
100 Washington Square East, New York, NY 10003, USA*

<sup>2</sup>*NASA, Goddard Institute for Space Studies, 2880 Broadway, New York, NY 10025, USA*

<sup>3</sup>*Carnegie Institution for Science, Department of Global Ecology, 260 Panama St.  
Stanford, CA 94305, USA*

## Abstract

We find that spectral analyses of the ages of the ten recorded major ocean anoxic events of the past 260 Ma reveal a strong spectral peak at 26.9 My significant at the ~95% confidence level. This cycle matches the periodicities of ~26 to 36 My detected in fluctuations in tectonics, sea levels and climate, in flood-basalt eruptions, and in biotic extinctions. The ages of eight of these anoxic events are correlated with concurrent episodes of extinctions of marine organisms. All ten anoxic intervals are closely associated with the ages of flood-basalt eruptions, suggesting causal connections through volcanic release of greenhouse gases resulting in severe hyperthermal intervals and hypoxia in the oceans.

## Introduction

Episodes of widespread hypoxia in the oceans have occurred from time to time during the last 260 My. These anoxic and euxinic intervals have been associated with hyperthermal climate events, and are suggested as a link between greenhouse gas emissions from flood-basalt volcanism and resulting marine-extinction episodes (e.g., Wignall et al., 2005; Wignall, 2015; Palfy and Smith, 2000; Palfy et al., 2001; Hotinski et al., 2001; Cao et al., 2009; Mehay et al., 2009; Bonis et al., 2010; Jenkyns, 2010; Ruhl, et al., 2011; Song et al., 2013; Sell et al., 2014; Tedeschi et al., 2017; B. Zhang et al., 2018; F. Zhang et al. 2018; Benton, 2018; Penn et al., 2018).

Large volumes of greenhouse gases (CO<sub>2</sub> and CH<sub>4</sub>) derived from the flood-basalt eruptions and from intrusive magmatic (large sills and dikes) interactions with carbon-rich country rocks (creating thermogenic methane) have apparently led to episodes of extremely warm global temperatures (Retallack, 1999; McElwain et al., 2005; Svensen et al., 2007; Schaller et al., 2011; Sun et al., 2012; Brand et al., 2012; Ernst and Youbi, 2017; Davies et al., 2017; Benton, 2018), and to warm, sluggish, stratified and poorly oxygenated oceans, culminating in widespread ocean hypoxia (Wignall, et al., 2005; Kiehl and Shields, 2005; Wignall, 2015; Ruhl and Kurschner, 2011; Caruthers et al., 2014; Clarkson et al., 2015; Baroni et al., 2018; Penn et al., 2018).

The warming would have also accelerated continental weathering (Retallack, 1999; Sheldon, 2005; von Strandmann, et al., 2013; Sun et al., 2018; F. Zhang et al., 2018), and increased the supply of phosphates, nitrates and other nutrients to oceanic surface waters via river runoff. This could have triggered unusually high export productivity, leading to greater oxygen demand in the deep ocean, and the spread of anoxic and even euxinic ocean conditions, leading to mass extinctions of marine life (Weissert et al., 1998; Bellanca et al., 2002; Handoh and Lenton, 2003; Scopelliti et al., 2004; Erba, 2004; Mort et al., 2007; Meyer et al., 2008; Cao et al., 2009; Owens et al., 2013; Ohkouchi et al., 20015; Coccioni et al., 2016; Them et al., 2018).

As marine-extinction events have been found to show evidence of an underlying 26 to 30 My periodicity (e.g., Raup and Sepkoski, 1986; Rampino and Caldeira, 2015), and flood-basalt eruptions might follow a similar underlying cycle (Rampino and Stothers, 1988), we decided to test for periodicity in the record of anoxic intervals.

### **Ocean anoxic events**

We compiled the record of major ocean anoxic events of the last 260 Ma from the literature (e.g., Jenkyns, 2010, 2018; Leckie et al., 2002; Handoh and Lenton, 2003; Sageman, 2009; Wignall, 2015; F. Zhang et al., 2018), re-dated to the latest timescale (Ogg et al., 2016) (Table 1). Ten well-defined episodes of widespread ocean anoxia are recorded (an average of one every 29 My) -- at 56 Ma (the Paleocene-Eocene Thermal Maximum); 66 Ma (the Cretaceous-Paleogene boundary); 93.9 Ma (OAE 2 – end-Cenomanian, the Bonarelli Event); ~122 Ma (OAE 1a – early Aptian, the Selli Event); 134.7 Ma (Valanginian, the Weissert Anoxic Event); 145 Ma (the end-

Jurassic anoxic event); 183.7 Ma (the Toarcian Anoxic Event); 201.4 Ma (the end-Triassic anoxic event); 251.9 Ma (the end-Permian “super-anoxic” event); and 259.8 Ma (the end-Guadalupian anoxic event) (Table 1). Eight of these ten anoxic events are correlated with concurrent episodes of extinctions of marine organisms (Table 1).

Major anoxic events may have lasted for more than a million years (Isozaki, 1997). The duration of OAE 2 (the Bonarelli Event) is estimated from several localities at up to 820 ka (Scopeletti et al., 2006; Li et al., 2017), and the duration of OAE 1a (the Selli Event) is roughly estimated at between 1 and 1.3 My (Li et al., 2008).

Several other brief ( $\leq 1$  My) hypoxic intervals, associated with hyperthermal events, but not with significant extinction pulses, occurred during the mid-Cretaceous (from the Albian to the Coniacian Stages) at ~113 Ma (OAE 1b; Level 113, Jacob Event, Monte Nerone Event); ~102 Ma (OAE 1c), ~100 Ma (OAE 1d, Piale Level); ~97 Ma (MCE, the mid-Cenomanian Event); and ~87 Ma (OAE 3) (Handoh and Lenton, 2003; Ingram et al., 1994; Coccioni and Galeotti, 2003; Mitchell et al., 2008) (Table 1). The earlier Faraoni Event in the latest Hauterivian Stage (~130 Ma) represents a brief dysoxic interval originally seen in the Italian Umbria-Marche Apennines (Coccioni et al., 1998; Baudin et al., 2002), but apparently found as far away as the central and northwestern Pacific (Follmi et al., 2012).

## Time-series analysis of ocean anoxic events

In order to evaluate the potential periodic nature of the major hypoxic events of the last 260 My (Table 1), we utilized the circular spectral analysis method first developed by Schuster, 1875) and von Mises (1918), and refined by Stothers (1991). The method was designed to test for cycles in a time series of discrete events without amplitude information (effectively, a time series of Dirac delta-functions), where at least some of the events in the time series are thought to represent an underlying periodic process with some superimposed noise, but where some of the events could be spurious and not related to the periodic process. This method effectively measures the degree of clustering of events when the dates of the events are mapped to a data modulus of the test period under consideration. It produces a normalized distance metric, which should be minimized at the preferred cycle. The method works well for time-series like ocean anoxic events, which lack amplitude information, may be a mixture of periodic and non-periodic events, and consist of unevenly spaced data.

For circular spectral analysis, a timeline is 'wrapped' around a circle, the circumference of which represents a trial period (Stothers, 1991). For each occurrence, we calculate a unit vector from the origin. A series that is not periodic will tend to plot randomly around the circle, regardless of trial period selected. A periodic series, however, will tend to form a cluster at one point on the circumference when the correct trial period  $P$  is selected. The angular location of the cluster relative to  $0^\circ$  (the present) gives the phase ( $t_0$ ).

The event times  $t_i$  are mapped onto a circle by conversion to angles  $a_i$  and  $b_i$  :

$$a_i = \sin 2\pi/P (t_i)$$

$$b_i = \cos 2\pi/P (t_i)$$

$$S = 1/N \sum_{i=1}^{N_i} (a_i) \quad (1)$$

$$C = 1/N \sum_{i=1}^{N_i} (b_i)$$

$$R = (S^2 + C^2)^{1/2}$$

109 where  $i$  ranges from 1 to  $N$  (the number of events), and  $P$  is the trial period.  $S$  and  $C$  are the  
110 summations,  $S = (\sum \sin a_i)/N$  and  $C = (\sum \cos b_i)/N$ .

111 Application of circular statistics leads to a mean vector magnitude,  $R = (S^2 + C^2)^{1/2}$  (a  
112 normalized measure of goodness of fit). The direction of the vector that minimizes the dispersion at  
113 the trial period  $P$  indicates the phase, which can be computed:  $t_0 = (P/2\pi) \tan^{-1}(S/C)$ , if  $C > 0$ , or as  
114  $t_0 = (P/2) + (P/2\pi) \tan^{-1}(S/C)$ , if  $C < 0$ . If  $R$  is plotted against  $P$ , then maximal values of  $R$  would  
115 correspond to periods in the series,  $t_1, t_2, \dots, t_N$ . If, however,  $t_1, t_2, \dots, t_N$  are randomly distributed,  
116 then  $(a_i, b_i)$  would define a random walk, and the sum  $R$  will be small.

117 In this method, the normalized distance metric does not have a direct interpretation in  
118 terms of statistical significance. To assess statistical significance, we address the question: What  
119 is the likelihood that a time series drawn at random from the universe of possible time series would  
120 have a smaller normalized distance metric at the test period than does the actual time series?

121  
122 To ensure that our results are a consequence of true periodicity and not of a characteristic  
123 recurrence interval, we constructed the set of test time series as follows. First, we calculated the  
124 length of time between each of the  $N$  events in the test time series, giving  $N - 1$  intervals. We then  
125 took a random permutation of these  $N - 1$  intervals and generated a time series of  $N$  events by  
126 taking the cumulative sum of this random permutation. Thus, we are testing against a universe of  
127 time series that contain the same set of intervals as the test time series, but permuted in a different  
128 order. This makes it clear that the periodicity is a consequence of the ordering of the intervals and  
129 not the statistical distributions of the intervals themselves.

130  
131 We compared the Stothers (1991) normalized distance metric calculated at each test  
132 period with the normalized distance metric computed for 100,000 pseudo-time series generated by  
133 the permutation approach described above, each having 10 events over an interval of 260 My (Fig.  
134 1). This significance test is powerful because the same set of intervals is present in the test time  
135 series and every one of the pseudo-time series, and the total length of the all of the pseudo-time  
136 series is identical to that of the test time series, eliminating artifacts associated with varying record  
137 lengths (Lutz, 1985) This significance test thus ascertains the likelihood that a random permutation  
138 of the same set of intervals would produce as strong evidence of periodicity as the time series

being tested. The 0.95, 0.99, and 0.999 confidence lines in Figure 1 represent the 95<sup>th</sup>, 99<sup>th</sup> and 99.9<sup>th</sup> percentile result of 100,000 random pseudo-data sets.

The most significant spectral peak in the spectrum of anoxic events for periods from 15 to 50 My falls at 26.9 My (~95% confidence) (Figure 1). *P*-values in Figure 2 represent the number of cases out of 100,000 Monte Carlo simulations that had higher scores in Stothers' test. The *P*-value of 0.05 means that of 100,000 Monte Carlo simulations only 5,000 cases had higher scores in Stothers' method. A high-frequency peak occurs at 12.6 My (relative power = 0.75) (Fig. 1). This is similar to a spectral peak seen in other geologic time series at about the same period, and may represent an independent climatic cycle (Boulila, 2019). It is, however, close to ½ the 26.9 My cycle.

## Flood-basalt eruptions, ocean hypoxia and extinction episodes

The link between ocean hypoxia and marine extinctions may come from the severe reduction of habitats for benthic and pelagic organisms as anoxic waters spread, from increases in toxic trace metals in sulfidic waters, (e.g., Hg, As, Cr) (Leary and Rampino, 1990; Sanei et al., 2012), and/or by release of poisonous H<sub>2</sub>S (Kump et al., 2005; Grice et al., 2005; Meyer et al., 2008; Penn et al., 2018) into the oceans and atmosphere. Release of H<sub>2</sub>S could also have damaged the ozone layer (Lamarque et al., 2007) affecting non-marine fauna and flora as well.

The 27 My cycle seen in anoxic events is similar to the periodicity reported in marine extinction events (Raup and Sepkoskit, 1986; Rampino and Caldeira, 2015), in episodes of flood-basalt volcanism (Rampino and Stothers, 1988; Rampino and Prokoph, 2013), and in tectonically-induced oscillations of sea level (Boulila, 2018). It is notable that all ten of the anoxic intervals in Table 1 are coincident with the ages of flood-basalt episodes. This suggests that periods of flood-basalt volcanism, and resulting hyperthermal-hypoxic ocean conditions are related to global tectonic episodes that affect global sea levels (Embry et al., 2018) and also climate through pulses of release of volcanic greenhouse gases (Muller and Dutkiewicz, 2018).

The apparently ubiquitous underlying ca. 30-My cycles in geologic, climatic and biotic events are most likely driven by internal Earth processes (Sheridan, 1987), perhaps modulated by

astrophysical factors such as pulses of heating during encounters with dark matter as the solar system oscillates through the galactic plane every ~30 Ma (Rampino, 2015; Abbas and Abbas, 1998). A similar underlying ~30 My periodicity has been reported in the ages of terrestrial impact structures, possibly from comet showers from the Oort Cloud generated from the same encounters with disc dark matter (Randall and Reece, 2014).

## . ACKNOWLEDGMENTS

We thank S. Abbas, M. Benton, C. Koeberl, and H. Jenkyns for helpful discussions, M.R.R. was funded through an NYU Research Challenge Grant.

## REFERENCES CITED

- Abbas, S., and Abbas, A., 1998, Volcanogenic dark matter and mass extinctions: *Astroparticle Physics*, v. 8, p. 317-320.
- Alvarez, L.W., Alvarez, W., Asaro, F., and Michel, H.V., 1980, Extraterrestrial cause for the Cretaceous-Tertiary extinction: *Science*, v. 208, p. 1095-1108.
- Baroni, I.R. et al., 2018, Ocean circulation in the Toarcian (Early Jurassic): A key control on deoxygenation and carbon burial on the European shelf: *Paleoceanography and Palaeoclimatology*, v. 33, p. 994-1022.
- Baudin, F., Cecca, F., Galeotti, S., and Coccioni, R., 2002, Palaeoenvironmental controls of the distribution of organic matter within a C<sub>org</sub>-rich marker bed (Faraoni level, uppermost Hauterivian, central Italy): *Eclogae geologicae Helvetica*, v. 95, p. 1-13.
- Bellanca, A., Erba, E., Neri, R., Premoli Silva, I., Sprovieri, M., Tremolada, F., and Verga, D., 2002, Palaeoceanographic significance of the Tethyan 'Livello Selli' (Early Aptian) from the Hybla Formation, northwestern Sicily: biostratigraphy and high-resolution chemostratigraphic records: *Palaeogeography, Palaeoclimatology, Palaeoecology*, v. 185, p. 175-196.
- Benca, J.P., Duijnste, I.A.P., and Looy, C.V., 2018, UV-B-induced forest sterility: Implications of ozone shield failure in Earth's largest extinction: *Science Advances*, v. 4, e1700618.
- Black, B.A., Lamarque, J., Shields, C.A., Elkins-Tanton, L.T., and Kiehl, J.T., 2014, Acid rain and ozone depletion from pulsed Siberian Traps magmatism: *Geology*, v. 42, p. 67-70.



199 Bonis, N.R., Ruhl, M., and Kurschner, W.M., 2010, Climate change driven black shale  
 200 deposition during the end-Triassic in the western Tethys: *Palaeogeography,*  
 201 *Palaeoclimatology, Palaeoecology*, v. 290, p. 151-159.

202 Boulila, S., 2019, Coupling between Grand cycles and Events in Earth's climate during the past  
 203 115 million years: *Scientific Reports*, v. 9, 327. Doi:10.1038/s41598-018-36509-7

204 Brand, U., Posenato, R., Came, R., Affek, H., Angiolini, L., Azmy, K., and Farabegoli, E.,  
 205 2012, The end-Permian mass extinction: A rapid volcanic CO<sub>2</sub> and CH<sub>4</sub>-climatic  
 206 catastrophe: *Chemical Geology*, v. 322-323, p. 121-144.

207 Caldeira, K. and Rampino, M.R., 1991, The mid-Cretaceous super plume, carbon dioxide, and  
 208 global warming: *Geophysical Research Letters*, v. 18, p. 987-990.

209 Cao, C., Love, G.D., Hays, L.E., Wang, W., Shen, S., and Summons, R.E., 2009,  
 210 Biogeochemical evidence for euxinic oceans and ecological disturbance presaging the  
 211 end-Permian mass extinction event: *Earth and Planetary Science Letters*, v. 281, p. 188-  
 212 201.

213 Clarkson, M.O., Kasemann, S.A., Wood, R.A., Lenton, T.M., Daines, S.J., Richoz, S.,  
 214 Ohnemueeller, F., Meixner, A., et al., 2015, Ocean acidification and the Permo-Triassic  
 215 mass extinction: *Science*, v. 348 p. 229-332.

216 Coccioni, R., and Galeotti, S., 2003, The mid-Cenomanian event: Prelude to OAE 2:  
 217 *Palaeogeography, Palaeoclimatology, Palaeoecology*, v. 190, p. 427-440..

218 Coccioni, R., Baudin, F., Cecca, F., Chiara, M., Galeotti, S., and Gardin, S., and Salvani, G., 1998,  
 219 Integrated stratigraphic, palaeontological, and geochemical analysis of the uppermost  
 220 Hauterivian Faraoni Level in the Fiume Bosso section, Umbria-Marche Apennines, Italy:  
 221 *Cretaceous Research*, v. 19, p. 1-23.

222 Day, M.O., Ramezani, J., Bowring, S., Sadler, P.M., Erwin, D.H., Abdala, F., and Rubidge, B.S.,  
 223 2015, When and how did the terrestrial mid-Permian mass extinction occur? Evidence  
 224 from the tetrapod record of the Karoo Basin, South Africa: *Proceedings of the*  
 225 *Royal Society B*, v. 282. 20150834.

226 Erba, E., Bartolini, A., and Larson, R.L., 2004, Valanginian Weissert oceanic anoxic event:  
 227 *Geology*, v. 32, p. 149-152

228 Follmi, K.B., et al., 2012, Bridging the Faraoni and Selli oceanic anoxic events: late  
 229 Hauterivian to early Aptian dysaerobic to anaerobic phases in the Tethys: *Climates of the*  
 230 *Past*, v. 8, p. 171-189.

231 Grice, K., Cao, C., Love, G.L., and Jin, Y., 2005, Photic zone euxinia during the Permian-Triassic  
 232 superanoxic event: *Science*, v. 307, p. 706-709.

233 Handoh, I.C., and Lenton, T.M., 2003, Periodic mid-Cretaceous oceanic anoxic events linked by  
 234 oscillations of phosphorus and oxygen biogeochemical cycles: *Global Biogeochemical*  
 235 *Cycles*, v. 14, 1092, doi:10.1029/2003GB002039

236 Isozaki, Y., 1997, Permo-Triassic boundary superanoxia and stratified superocean:  
 237 *Records from lost deep sea: Science*, v. 278, p. 235-238.

238 Jenkyns, H. C., 2010, Geochemistry of oceanic anoxic events: *Geochemistry, Geophysics,*  
 239 *Geosystems*, v. 11, p. 1-30.

240 Jenkyns, H.C., 2018, Transient cooling episodes during Cretaceous Oceanic Anoxic Events with  
 241 special reference to OAE 1a (Early Aptian): *Philosophical Transactions of the Royal*  
 242 *Society A*, v. 376, 20170073.

243 Keller, G., 2008, Cretaceous climate, volcanism, impacts, and biotic effects: *Cretaceous*  
 244 *Research*, v. 29, p. 754-771.

245 Kump, L.R., Pavlov, A., and Arthur, M.A., 2005, Massive release of hydrogen sulfide to the  
 246 surface ocean and atmosphere during intervals of oceanic anoxia: *Geology*, v. 33, p. 397–  
 247 400.

248 Lamarque, J. -F., Kiehl, J.T., and Orlando, J.J., 2007, Role of hydrogen sulfide in a Permian-  
 249 Triassic boundary ozone collapse: *Geophysical Research Letters*, v. 34, L02801.

250 Leary, P.N., Rampino, M.R., 1990, A multi-causal model of mass extinctions: Increase in trace  
 251 metals in the oceans, In: Kauffman, E.G., and Walliser, O.H., eds., *Extinction Events in*  
 252 *Earth History*: Berlin, Springer-Verlag, p. 45-55.

253 Leckie, R.M., Bralower, T.J., and Cashman, R., 2002, Oceanic anoxic events and plankton  
 254 evolution: biotic response to tectonic forcing during the mid-Cretaceous: *Paleoceanography*,  
 255 v. 17, p. 1-29.

256 Lutz, T.M., 1985, The magnetic reversal record is not periodic: *Nature*, v. 317, p. 404-407.

257 McElwain, J.C., Wade-Murphy, J., and Hesselbo, S.P., 2005, Changes in carbon dioxide during an  
 258 oceanic anoxic event linked to intrusion of Gondwana coal: *Nature*, v. 435, p. 479-482.

259 Mehay, S., Keller, C.E., Bernasconi, S.M., Weissert, H., Erba, E., Bottini, C., and Hochuli, P.A.,  
 260 2009, A volcanic CO<sub>2</sub> pulse triggered the Cretaceous Anoxic Event 1a and a  
 261 biocalcification crisis: *Geology*, v. 37, p. 819-822.

262 Metcalfe, I., Crowley, J.L., Nicoll, R.S., and Schmitz, M., 2015, High-precision U-Pb CA-TIMS  
 263 calibration of Middle Permian to Lower Triassic sequences, mass extinction and extreme  
 264 climate-change in eastern Australian Gondwana: *Gondwana Research*, v. 28, p. 61-81.

265 Meyer, K.M., Kump, L.R., and Ridgwell, A., 2008, Biogeochemical controls on photic-zone euxinia  
 266 during the end-Permian mass extinction: *Geology*, v. 36, p. 747-750.

267 Mitchell, R.N., Bice, D.M., Montanari, A., Cleaveland, L.C., Christianson, K.T., Coccioni, R., and  
 268 Hinnov, L.A., 2008, Oceanic anoxic cycles? Orbital prelude to the Bonarelli Level (OAE 2):  
 269 *Earth and Planetary Science Letters*, v. 267, p. 1-16.

270 Mort, H., Jacquat, O., Adatte, T., Steinmann, P., Follmi, K., Matera, V., Berner, Z., and Stuben, D.,  
 271 2007, The Cenomanian/Turonian anoxic event at the Bonarelli Level in Italy and Spain:  
 272 enhanced productivity and/or better preservation? *Cretaceous Research*, v. 28, p. 597-  
 273 6123.

274 Ogg, J.G., Ogg, G.M., and Gradstein, F.M., 2016, *A Concise Geologic Time Scale 2016*,  
 275 Elsevier, Amsterdam.

276 Ohkouchi, N., Kuroda, J., and Taira, A., 2015, The origin of Cretaceous black shales: a change in  
 277 the surface ocean ecosystem and its triggers: *Proceedings of the Japanese Academy*,  
 278 *Series B*, v. 91, p. 273-291.

279 Onoue, T., Sato, H., Yamashita, D., Ikehara, M., Yasukawa, K., Fujinaga, K., Kato, Y., and  
 280 Matsuoka, A., 2016, Bolide impact triggered the Late Triassic event in equatorial  
 281 Panthalassa: *Scientific Reports* 6, 29609, doi: 10.1038/srep29609.

282 Owens, J.D., Gill, B.C., Jenkyns, H.C., Bates, S.M., Severmann, S., Kuypers, M.M.M.,  
 283 Woodfine, R.G., and Lyons, T.W., 2015, Sulfur isotopes track the global extent and  
 284 dynamics of euxinia during the Cretaceous Oceanic Anoxic Event 2: *Proceedings of the*  
 285 *National Academy of Sciences of the United States of America*, v. 110, p. 18407-18412.

286 Palfy, J., and Smith, P.L., 2000, Synchrony between Early Jurassic extinction, oceanic anoxic  
 287 event, and the Karoo-Ferrar flood basalt volcanism: *Geology*, v. 28, p. 747-750.

288 Palfy, J., Demeny, A, Haas, J., Hetenyi, M., Orchard, M.J., Veto, I., et al., 2001, Carbon isotope  
 289 anomaly and other geochemical changes at the Triassic-Jurassic boundary from a marine  
 290 section in Hungary: *Geology*, v. 29, p. 1047-1050.

291 Penn, J.L., Deutsch, C., Payne, J.L., and Sperling, E.A., 2018, Temperature-dependent hypoxia  
 292 explains biogeography and severity of end-Permian mass extinction: *Science*, v. 362,  
 293 eaat1327 (2018)

294 Prokoph, A., Rampino, M.R., and El Bilali, H., 2004, Periodic components in the diversity of  
 295 calcareous plankton and geologic events over the past 230 Myr: *Palaeogeography*,  
 296 *Palaeoclimatology*, *Palaeoecology*, v. 207, p. 105-125.

297 Rampino, .R., 2001, Galactic triggering of periodic comet showers and mass extinctions on Earth,  
 298 In: Marov, MY, and Rickman, H., eds., *Collisional Processes in the Solar System*, Kluwer,  
 299 Dordrecht, p. 103-120.

300 Rampino, M.R., 2015, Disc dark matter in the Galaxy and potential cycles of extraterrestrial  
 301 impacts, mass extinctions and geological events: *Monthly Notices of the Royal*  
 302 *Astronomical Society*, v. 448, p. 1816-1820.

303 Rampino, M.R., and Caldeira, K., 1992, Episodes of terrestrial geologic activity during the past  
 304 260 million years: A quantitative approach: *Celestial Mechanics and Dynamical*  
 305 *Astronomy*, v. 54, p. 143-159.

306 Rampino, M.R., and Caldeira, K., 1993, Major episodes of geologic change: correlations, time  
 307 structure and possible causes: *Earth and Planetary Science Letters*, v. 114, p. 215-227.

308 Rampino, M.R. and Caldeira, K., 2018, Comparison of the ages of large-body impacts, flood–  
 309 basalt eruptions, ocean anoxic events and extinctions over the last 260 million years: A  
 310 statistical study: *International Journal of Earth Sciences*, DOI: 10.1007/s00531-017-1513-  
 311 6

312 Rampino, M.R., and Stothers, R.B., 1988, Flood basalt volcanism during the past 250 million years:  
 313 *Science*, v. 241, p. 663-668.

314 Rampino, M.R., Caldeira, K., and Prokoph, A., 2019, What causes mass extinctions? Large  
 315 asteroid/comet impacts, flood-basalt volcanism, and ocean anoxia—Correlations and  
 316 cycles: *Geological Society of America Special Paper* 542, p. 1-32.

317 Randall, L., and Reece, M., 2014, Dark matter as a trigger for periodic comet showers: *Physical*  
 318 *Review Letters*, v. 112: 161301.

319 Raup, D.M., and Sepkoski, J.J., Jr., 1986, Periodic extinctions of families and genera: *Science*, v.  
320 231, p. 833-836.

321 Retallack, G.J., 1999, Postapocalyptic greenhouse paleoclimate revealed by earliest Triassic  
322 paleosols in the Sydney Basin, Australia: *Geological Society of America Bulletin*, v. 111, p.  
323 52-70.

324 Retallack, G.J., Metzger, C.A., Greaver, T., Jahren, A.H., Smith, R.M.H., and Sheldon, N.D.,  
325 2006, Middle-Late Permian mass extinction on land: *Geological Society of America*  
326 *Bulletin*, v. 118, p. 1398-1411.

327 Ruhl, M., and Kurschner, W.M., 2011, Multiple phases of carbon cycle disturbance from large  
328 igneous province formation at the Triassic-Jurassic transition: *Geology*, v. 39, p. 431-434.

329 Sageman, B., 2009, Ocean anoxic events, In: Gornitz, V., ed., *Encyclopedia of Paleoclimatology*  
330 *and Ancient Environments*: Dordrecht, Springer, p. 626-629.

331 Schulte, P., et al., 2010, The Chicxulub asteroid impact and mass extinction at the Cretaceous-  
332 Paleogene boundary: *Science*, v. 327, p. 1214-1218.

333 Schuster, A., 1897, On lunar and solar periodicities of earthquakes: *Proceedings of the Royal*  
334 *Society of London*, v. 61, p. 455-465. doi:10.1098/rspl.1897.0060.

335 Scopelliti, G., Bellanca, A., Coccioni, R., Luciani, V., Neri, R., Baudin, F., Chiari, M., and  
336 Marcucci, M., 2004, High-resolution geochemical and biotic records of the Tethyan  
337 'Bonarelli Level' (OAE 2, latest Cenomanian) from the Calabianca-Guidaloca composite  
338 section, northwestern Sicily, Italy: *Palaeogeography, Palaeoclimatology, Palaeoecology*,  
339 v. 208, p. 293-317.

340 Sell, B., et al., 2014, Evaluating the temporal link between the Karoo LIP and climatic-biologic  
341 events of the Toarcian Stage with high-precision U-Pb geochronology: *Earth and*  
342 *Planetary Science Letters*, v. 408, p. 48-56.

343 Sepkoski, J.J., Jr., 1989, Periodicity in extinction and the problem of catastrophism in the history of  
344 life: *Journal of the Geological Society, London*, v. 146, p. 7-19.

345 Sheldon, N.D., 2005, Abrupt chemical weathering increase across the Permian-Triassic boundary:  
346 *Palaeogeography, Palaeoclimatology, Palaeoecology*, v. 231, p. 315-321.

347 Sheridan, R., 1987, Pulsation tectonics as the control of long-term stratigraphic cycles:  
348 *Paleoceanography*, v. 2, p. 97-118.

349 Song, H., Wignall, P.B., Chu, D., Tong, J., Sun, Y., Song, H., He, W., and Tian, L., 2014,  
 350 Anoxia/high temperature double whammy during the Permian-Triassic marine crisis and its  
 351 aftermath: *Scientific Reports*, v. 4, 4132. DOI: 10.1038/srep04132.  
 352 Stothers, R.B., 1991, Linear and circular digital spectral analysis of serial data: *The Astronomical*  
 353 *Journal*, v. 375, p. 423-426.  
 354 Stothers, R.B., 1998, Galactic disc dark matter, terrestrial impact cratering and the law of large  
 355 numbers: *Monthly Notices of the Royal Astronomical Society*, v. 300, p. 1098-1104.  
 356 Sun, J., Ni, X., Bi, S., Wu, W., Ye, J., Meng, J., and Windley, B.F., 2014, Synchronous turnover  
 357 of flora, fauna, and climate at the Eocene–Oligocene Boundary in Asia: *Scientific Reports*,  
 358 v. 4, 7463.  
 359 Sun, Y., Joachimski, M.M., Wignall, P.B., Yan, C., Chen, Jiang, H., Wang, I. et al., 2012, Lethally  
 360 hot temperatures during the Early Triassic greenhouse: *Science*, v. 338, p. 366-370.  
 361 Tedeschi, L.R., Jenkyns, H.C., Robinson, S.A., Sanjines, A.E.S., Viviers, M.C., Quintaes,  
 362 C.M.S.P., and Vazquez, J.C., 2017, New age constraints on Aptian evaporites and  
 363 carbonates from the South Atlantic: Implications for Oceanic Anoxic Event 1a: *Geology*, v.  
 364 45, p. 543-546.  
 365 Them, T.R., II. et al., 2018, Thallium isotopes reveal protracted anoxia during the Toarcian (Early  
 366 Jurassic) associated with volcanism, carbon burial, and mass extinction: *Proceedings of*  
 367 *the National Academy of Sciences of the United States of America*, 2018033478.  
 368 doi:10.1073/pnas.1803478115.  
 369 Toon, O.B., Bardeen, C., and Garcia, R., 2016, Designing global climate and atmospheric  
 370 chemistry simulations for 1 and 10 km diameter asteroid impacts using the properties of  
 371 ejecta from the K-Pg impact: *Atmospheric Chemistry and Physics*, v. 16, 13185-13212.  
 372 von Mises, R., 1918, Über die "Ganzzahlligkeit" der Atomgewichte und verwandte Fragen:  
 373 *Physic Zeitschrift*, v. 19, p. 490-500.  
 374 von Strandmann, P.A.E., Jenkyns, H.C., and Woodfine, R.G., 2013, Lithium isotope  
 375 evidence for enhanced weathering during Ocean Anoxic Event 2: *Nature Geoscience*, v.  
 376 6, p. 668-672.  
 377 Weissert, H., Lini, A., Follmi, K.B., and Kuhn, B., 1998, Correlation of Early Cretaceous carbon  
 378 isotope stratigraphy and platform drowning events: a possible link:  
 379 *Palaeogeography, Palaeoclimatology, Palaeoecology*, v. 137, p. 189-203.

- Wignall, P.B., 2015, The Worst of Times: How Life Survived Eighty Million Years of Extinctions: Princeton, Princeton University Press.
- Wignall, P.B., Newton, R.J., and Little, C.T.S., 2005, The timing of paleoenvironmental change and cause-and-effect relationships during the Early Jurassic mass extinction in Europe: American Journal of Science, v. 305, p. 1014-1032.
- Zaffani, M., Agnini, C., Concheri, G., Godfrey, L., Katz, M., Maron, M., and Rigo, M., 2017, The Norian "chaotic carbon interval": New clues from  $\delta^{13}\text{C}_{\text{org}}$  record of the Lagonero Basin (southern Italy): Geosphere, v. 13, doi: 10.1130/GES01459.1.
- Zhang, B., Yao, S., Hu, W., Ding, H., and Liu, B., 2018, Development of a high-productivity and anoxic-euxinic condition during the late Guadalupian in the Lower Yangtze region: Implications for the mid-Capitanian extinction event: Palaeogeography, Palaeoclimatology, Palaeoecology, DOI: 10.1016/j.palaeo.2018.01.021.
- Zhang, F., et al., 2018, Multiple episodes of extensive marine anoxia linked to global warming and continental weathering following the latest Permian mass extinction: Science Advances, v. 4, e1602921.
- Zhu, D.-C., et al., 2009, The 132 Ma Comei-Bunbury large igneous province: Remnants identified in present-day southeastern Tibet and southwestern Australia: Geology, v. 37, p. 581-585.

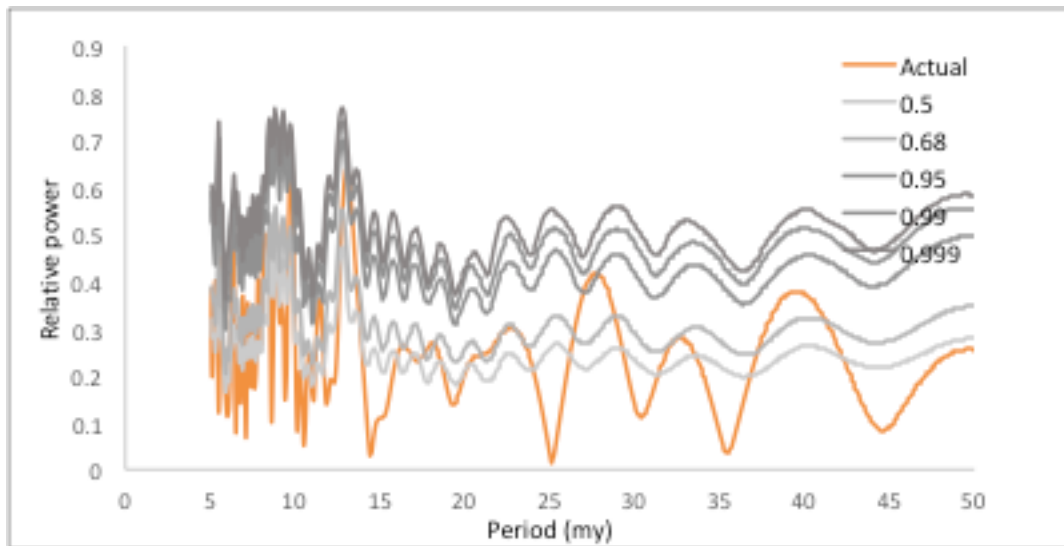
## Figure Captions

Figure 1. Power spectrum of 10 major anoxic intervals of the past 260 My (Table 1) for periods of 5 to 50 My based on the circular spectral analysis method of Stothers (1991). A significant (95% confidence) occurs at 26.9 My.

Figure 2. *P*-values for 10 major anoxic intervals over the past 260 My (Table 1) for periods from 5 to 50 My using the statistical method of Stothers (1991). The peak at 26.9 My is statistically significant ( $<0.05$ ).



# Figure 1





# Figure 2

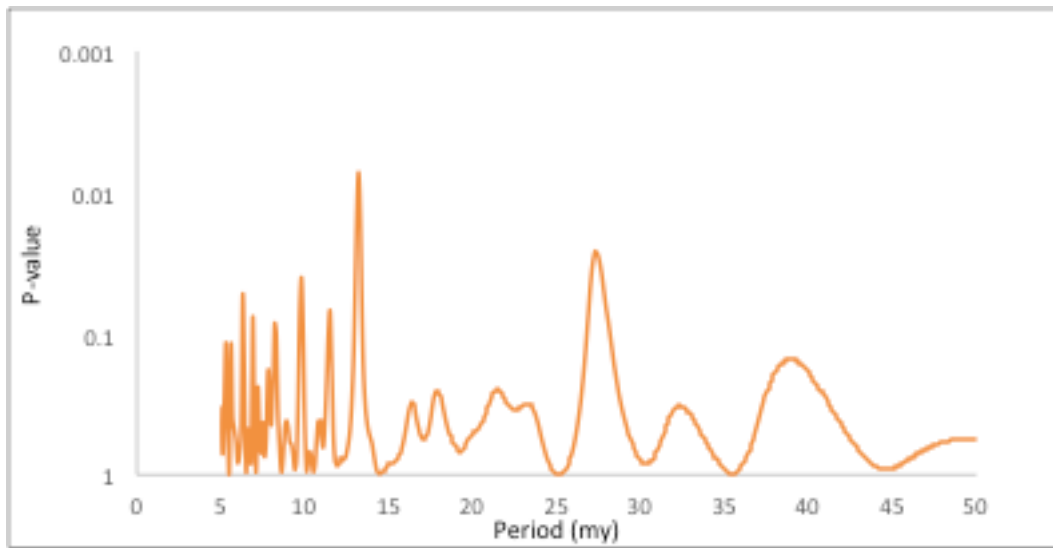




TABLE 1. Ocean anoxic events of the last 260 Ma, episodes of marine extinctions, flood-basalt eruptions, and stratigraphic Hg anomalies (for references see text).

Ocean Anoxic Events	Age (Ma)	Marine Extinction Episode	Flood Basalt	Age (Ma)	Hg Anomaly
PETM	56	PETM	NAIP	55.6, 61.9	Yes
K-Pg	66	Yes	Deccan	66.3 $\pm$ 0.03	Yes
End-Cenomanian (OAE 2)	93.9	Yes	Madagas/Carib	92 to 94	Yes
Early Aptian (OAE 1a)	~120	Yes	Rajmahal/ OJP/Ker	~120	Yes
End-Hauterivian (Weissert)	134.7	----	Parana/Etendeka	134.3 $\pm$ 0.8	Yes
End-Jurassic	145	Yes	Shatsky Rise	144.4 $\pm$ 1.0	----
Toarcian	183.7	Yes	Karoo/Ferrar	183 $\pm$ 1	Yes
End-Triassic	201.4	Yes	CAMP	201.5 $\pm$ 0.05	Yes
End-Permian	251.9	Yes	Siberian	251.9 $\pm$ 0.07	Yes
End-Guadalupian	259.8	Yes	Emeishan	259.6 $\pm$ 0.5	Yes
<u>Minor OAEs</u>					
OAE 1b	113	No	Kerguelen (?)	?	Yes
OAE 1c	102	No	No		----
OAE 1d	100	No	No		----
Mid-Cenomanian Event (MCE)	97	No	No		----
OAE 3	87	No	No		----
Faraoni	130	No	Comei-Bunbury	131.5 $\pm$ 0.8	----